NANO LETTERS
Letter
Cite This: Nano Lett. XXXX, XXX, XXX−XXX
pubs.acs.org/NanoLett

Excitation and Emission Transition Dipoles of Type-II Semiconductor Nanorods

Subhabrata Ghosh,[†] Anna M. Chizhik,[†] Gaoling Yang,[‡] Narain Karedla,[#] Ingo Gregor,[†] Dan Oron,[‡] Shimon Weiss,[§,∥,⊥,#] Jörg Enderlein,[†] and Alexey I. Chizhik*[,†]

[†]Georg August University Göttingen, Third Institute of Physics, Göttingen 37077, Germany
[‡]Department of Physics of Complex Systems, Weizmann Institute of Science, Rehovot 76100, Israel
[§]Department of Chemistry and Biochemistry, University of California Los Angeles, Los Angeles, California 90095, United States
[∥]California NanoSystems Institute, University of California Los Angeles, Los Angeles, California 90095, United States
[⊥]Department of Physiology, University of California Los Angeles, Los Angeles, California 90095, United States
[#]Department of Physics, Institute for Nanotechnology and Advanced Materials, Bar-Ilan University, Ramat-Gan 52900, Israel

Supporting Information

ABSTRACT: The mechanisms of exciton generation and recombination in semiconductor nanocrystals are crucial to the understanding of their photophysics and for their application in nearly all fields. While many studies have been focused on type-I heterojunction nanocrystals, the photophysics of type-II nanorods, where the hole is located in the core and the electron is located in the shell of the nanorod, remain largely unexplored. In this work, by scanning single nanorods through the focal spot of radially and azimuthally polarized laser beams and by comparing the measured excitation patterns with a theoretical model, we determine the dimensionality of the excitation transition dipole of single type-II nanorods. Additionally, by recording defocused patterns of the emission of the same particles, we measure their emission transition dipoles. The combination of these techniques allows us to unambiguously deduce the dimensionality and orientation of both excitation and emission transition dipoles of single type-II semiconductor nanorods. The results show that in contrast to previously studied quantum emitters, the particles possess a 3D degenerate excitation and a fixed linear emission transition dipole.

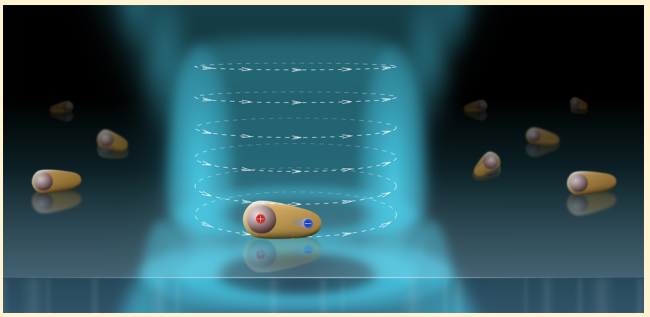

KEYWORDS: *cylindrical vector beams, higher order laser modes, nanorods, optical transition dipole, quantum dot, semiconductor nanocrystal*

After more than three decades since the discovery of luminescent semiconductor nanocrystals, they still have unexplored and intriguing photophysical properties that have been unimaginable before. Their high brightness, photostability, and tunability of emission and absorption properties based on their size and composition make them a superior choice for numerous applications. Synthesis of type-II nanorods, where the electron is delocalized in the particle's shell, is of great fundamental interest and has opened new perspectives for local voltage sensing at the nanometer scale[1−5] or in optical gain studies.[6] Despite the progress in their controlled synthesis and characterization, some of their photophysical properties remain unknown. In particular, the generation and recombination of excitons in type-II nanorods is one of the key mechanisms that remains unexplored.

Experimentally, these processes can be characterized by measuring excitation and emission transition dipoles of single particles. Dimensionality and orientation of the excitation transition dipole determines the excitation efficiency of the particles using light, depending on its polarization, or via energy transfer from another quantum emitter. The parameters of the emission transition dipole define the polarization of emitted light from a particle, playing an important role in use of nanocrystals as donors in FRET pair or as emitters of light.

It has been shown that shape and composition of semiconductor nanostructures can change the dimensionality of their emission and excitation transition dipole moments. As was theoretically predicted by Efros,[7] the emission transition dipole of a spherical CdSe nanocrystal is degenerate in two dimensions. Such a system is characterized by a unique "dark axis" that is oriented normal to the transition dipole plane, and which does not couple to the light field. This has been experimentally shown using polarization microscopy[8,9] and,

Received: November 21, 2018
Revised: January 28, 2019
Published: February 5, 2019

DOI: 10.1021/acs.nanolett.8b04695
Nano Lett. XXXX, XXX, XXX−XXX

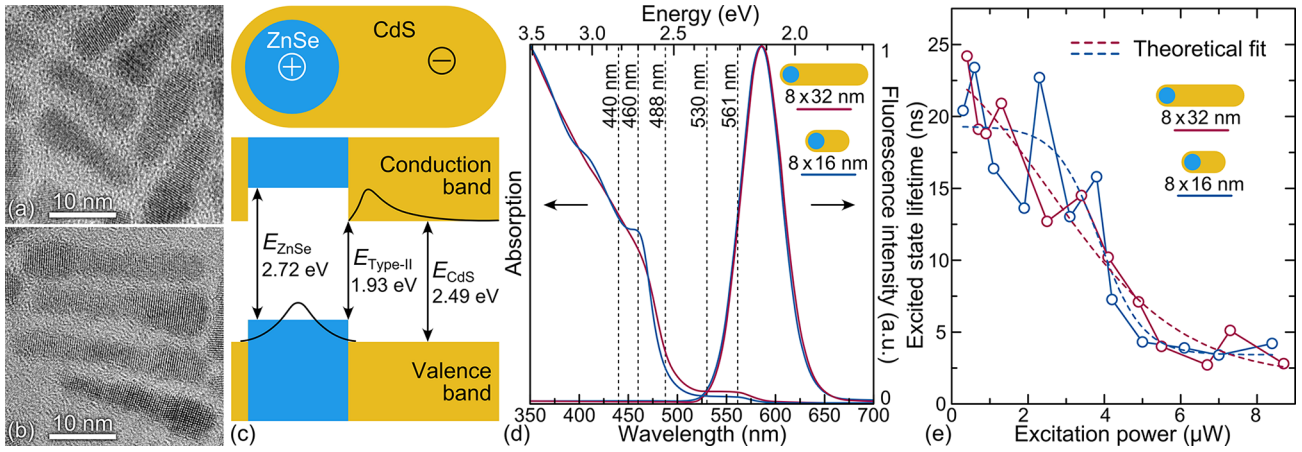

Figure 1. Transmission electron microscopy images of 8 × 32 nm (a) and 8 × 16 nm (b) ZnSe/CdS nanorods. (c) Schematic of the ZnSe/CdS core−shell nanorod and its type-II conduction and valence band structure. The band gaps for ZnSe and CdS are given for bulk material. (d) Absorption and fluorescence spectra of 8 × 32 and 8 × 16 nm ZnSe/CdS nanorods. Vertical dashed lines indicate the excitation wavelengths used in this study. (e) Dependence of the excited state lifetime of ZnSe/CdS nanorods on the intensity of excitation light (see main text for further details).

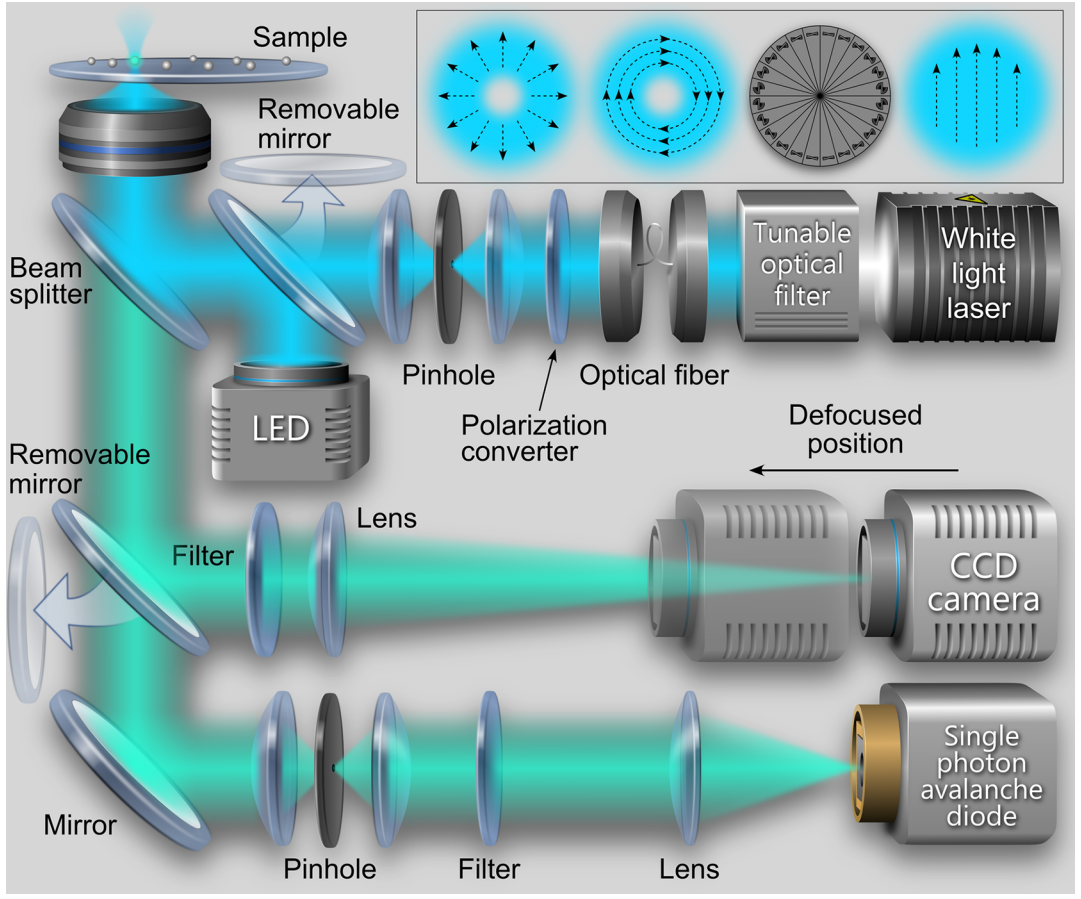

Figure 2. Scheme of the microscope that combines a scanning confocal and wide field imaging modes. The excitation line for the confocal part is equipped with a polarization converter that allows one to obtain a radially or azimuthally polarized laser beam. The inset shows (right to left): a cross-section of a linearly polarized Gaussian beam, a scheme of a polarization converter, a cross-section of an azimuthally polarized laser beam, and a cross-section of a radially polarized laser beam. Note that the focused radially polarized laser beam has a longitudinal component in the center of the beam (see the Supporting Information for further details).

later, by several groups using defocused wide field fluorescence imaging.[10−12] By rotating the excitation polarization, Bawendi and co-workers observed a weak excitation polarization dependence, which was attributed to simultaneous excitation of multiple overlapping electronic states, decreasing the degree of polarization.[8] Later, it was shown that the excitation transition dipole moment of a spherical CdSe/ZnS quantum dot is degenerate in three dimensions.[13] Changing the shape of

DOI: 10.1021/acs.nanolett.8b04695
Nano Lett. XXXX, XXX, XXX−XXX

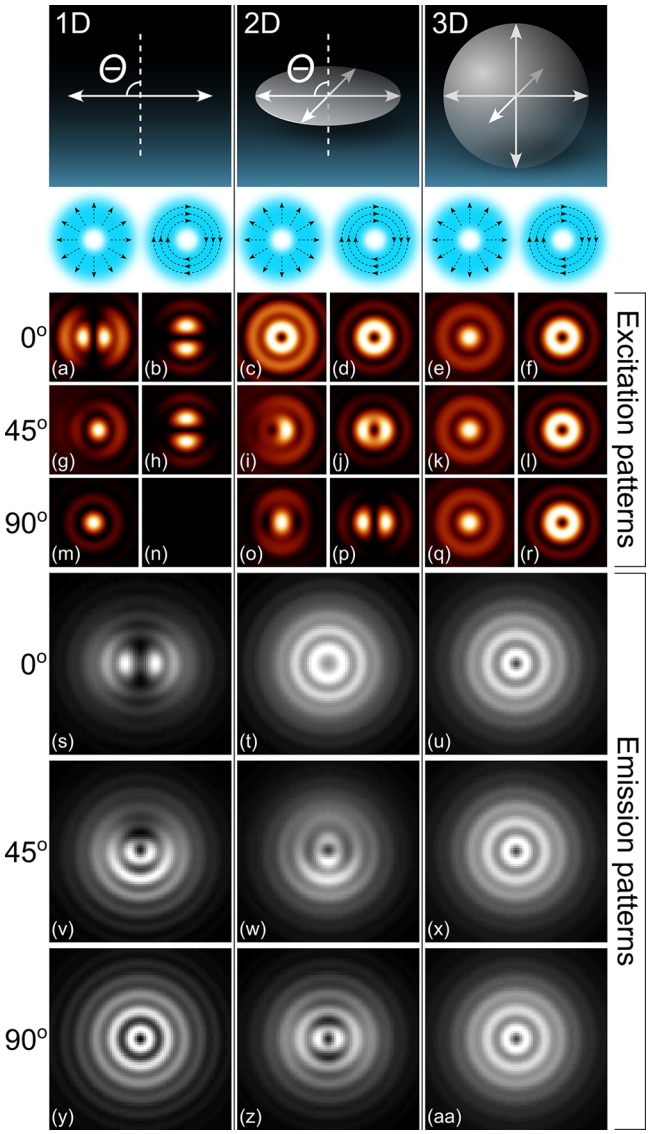

Figure 3. Theoretical excitation (a–r) and emission (s–aa) patterns of a single quantum emitter that has various orientations and degeneracies of transition dipole moments. The patterns were modeled according to the schemes shown on top of the figure for 500 nm excitation and 600 nm emission wavelengths. Modulation of the excitation wavelength from 440 to 561 nm slightly changes the size of the excitation patterns while keeping its shape the same. The shape and size of the emission patterns remain the same independently of excitation wavelength.

type-I heterojunction nanocrystals resulted in the change of their emission transition dipole dimensionality from one dimension for nanorods[14] to two dimensions for nanoplatelets.[15]

Here, we measure the dimensionality and orientation of both emission and excitation transition dipoles of single type-II nanorods. The excitation transition dipole is measured by scanning individual nanorods though the focal area of azimuthally and radially polarized laser beams (so-called donut modes). The measurement of the emission transition dipole is done using defocused imaging of the same single nanoparticles. In contrast to other commonly used techniques, like rotation of a linear polarizer in front of a photodetector,[8,9,15] both of these methods allow one to unambiguously determine both the dimensionality and 3D orientation of the transition dipoles.[10,13,16,17]

We studied 8 × 16 and 8 × 32 nm CdS nanorods with a ZnSe spherical core inside that form a nanostructure with a type-II potential profile (Figure 1a–c). This system has two distinctive regimes of light absorption.[14,18] The high-energy absorption above 2.65–2.7 eV is associated with the electronic transitions involving either the ZnSe core or the CdS shell. The absorption feature at the red edge of this spectral region can be assigned to the first electronic transition in the CdS core and is shifted toward higher energy in comparison with bulk value of 2.49 eV due to size quantization. The absorption tail at the red side of the spectrum lies below the bulk bandgaps of both materials and is related to the indirect type-II band gap of the system.[14] To study the transition dipole moments in different absorption regimes, we did measurements at five different excitation wavelengths that cover the energy range from 2.21 to 2.82 eV (Figure 1d).

To minimize the probability of the multiexciton generation, we studied the dependence of the excited state lifetime of single nanorods on the intensity of excitation light.[19] The measurement was done at a 440 nm excitation wavelength, where the absorption probability is maximized as compared to the other excitation wavelengths used. The light intensity was measured right before a 1.49 NA objective lens and corresponds to the linearly polarized laser beam that is filling, but not exceeding, the back aperture of the lens. As shown in Figure 1e, an increase of excitation light intensity leads to a decrease of the excited state lifetime of nanorods that is caused by trapping of excessive charges that are generated inside the nanorod and, as a result, an increase of probability of the nonradiative Auger recombination. Along with decreased lifetime values, it leads to a drop of fluorescence intensity and quantum yield of the emitter. Fitting the measured curves with a modified sigmoid function showed *x*-values of the midpoint at 3.9 and 2.6 microWatts for the 8 × 16 and 8 × 32 nm nanorods, respectively. The lower midpoint for the elongated rods can be explained by its higher absorption cross-section that leads to more efficient multiexciton generation at lower excitation light intensities as compared to shorter nanorods. All the studies of the transition dipole were done at excitation intensities not exceeding the above values.

Figure 2 shows a schematic of a microscope that combines both confocal scanning and wide field modes. The former allows one to measure single nanoparticle excitation patterns by scanning it through focal areas of azimuthally or radially polarized beams. The donut modes are obtained by transmitting a linearly polarized Gaussian beam through a liquid crystal polarization converter. Use of both azimuthal and radial modes allows one to unambiguously attribute an obtained excitation pattern to one of the possible dimensionalities and three-dimensional orientations of the excitation transition dipole moment.

The wide field mode of the microscope was used for measuring defocused emission patterns of single nanorods. By defocusing either the objective lens toward the sample or the chip of the camera by the corresponding distance, one observes peculiar emission patterns instead of a normal point spread function. The shape of the pattern allows one to retrieve information about the dimensionality and orientation of the emission transition dipole moment of the emitter. Excitation of nanorods for defocused imaging was done using unpolarized

DOI: 10.1021/acs.nanolett.8b04695
Nano Lett. XXXX, XXX, XXX–XXX

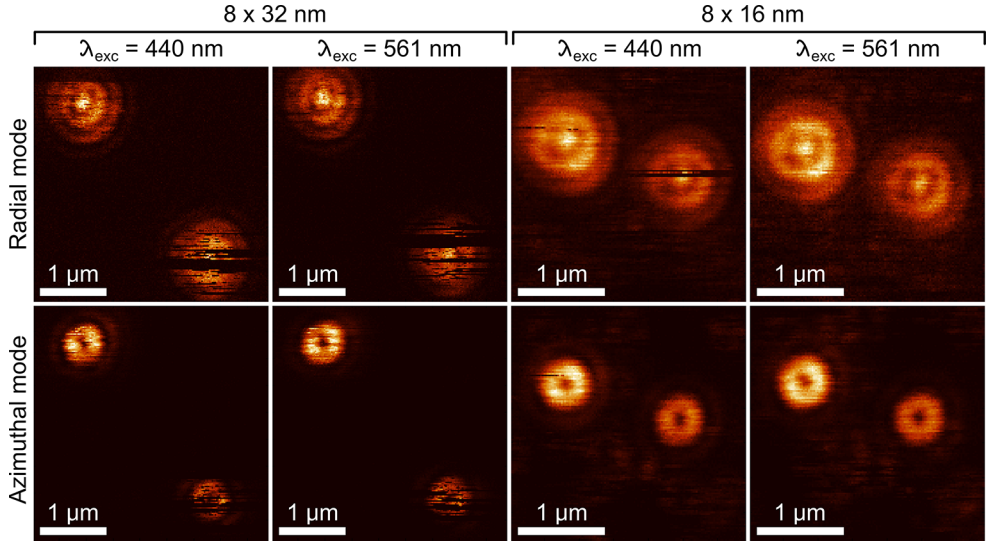

Figure 4. Experimental excitation patterns of ZnSe/CdS nanorods that were obtained using 440 and 561 nm excitation wavelengths using azimuthally and radially polarized laser beams. The dark lines correspond to the off state of the particles during the confocal scanning process. The excitation patterns that were obtained at other excitation wavelengths that were used in this study have the same shape except for the stochastic distribution of the fluorescence blinking events. All the patterns correspond to a three-dimensional degenerate excitation transition dipole, see Figure 3(a–r).

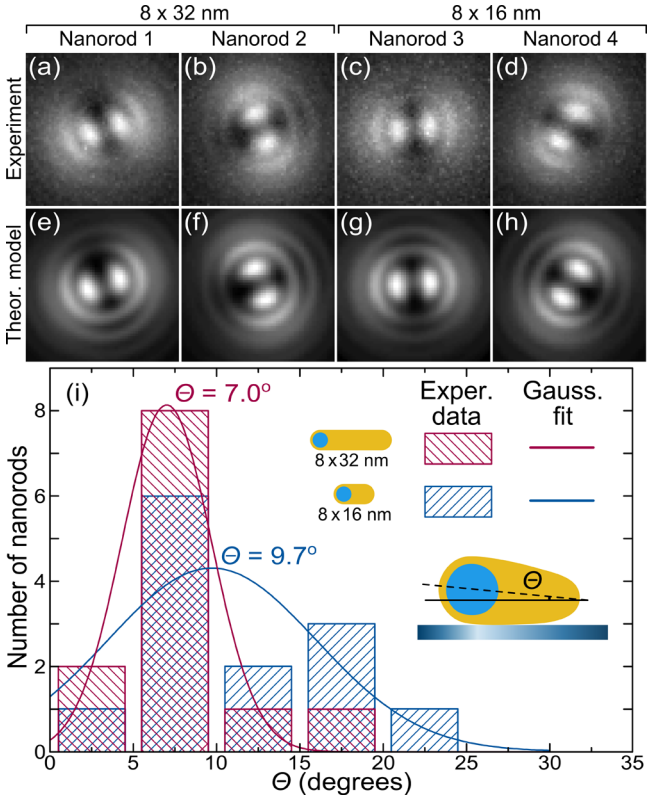

Figure 5. (a–d) Experimental defocused images that were measured in the wide field mode at 440 nm excitation wavelength. The patterns obtained at other excitation wavelengths that were used in this study have an identical shape. (e–h) Theoretical fit of the measured patterns. All the fits correspond to a fixed linear emission transition dipole, see Figure 3(s–aa). (i) Histogram of the out of plane angles that were obtained by fitting experimental emission patterns. The solid curves are Gaussian fits that have the maximum at 9.7° and 7.0° and full width at half maxima 14.8° and 6.3° for 8 × 16 and 8 × 32 nm nanorods, respectively.

light from a light emitting diode (LED) source to avoid selective excitation of emitters with certain polarization. To keep the same excitation wavelength and excitation intensity for wide field and confocal modes, the light from LEDs was transmitted through the same cleanup filters that were used for the laser. The excitation density for wide field imaging was adjusted such that single nanorod emission patterns had the same average intensity as upon excitation with a laser.

A prerequisite for characterization of excitation and emission transition dipoles of a quantum emitter using donut modes and defocused imaging is the modeling of the fluorophore's excitation and emission patterns. Figure 3 shows excitation and emission patterns of a single quantum emitter that has different a dimensionality and orientation of transition dipoles. The patterns were calculated according to the scheme shown on top of the figure and according to the experimental conditions and parameters of the microscope that were used in the measurements. The striking difference of the excitation and emission patterns allows one to unambiguously distinguish different dimensionalities and orientations of transition dipoles. It should be noted that in contrast to other techniques, such as rotation of a linear polarizer in front of a detector or use of only the azimuthal mode, these techniques allow one to determine not only orientation of transition dipoles within the sample plane but also the out-of-plane tilt of a dipole.

Figure 4 shows excitation dipoles obtained by scanning single nanorods through the focal areas of a radially and azimuthally polarized laser beam at the shortest (440 nm) and longest (561 nm) excitation wavelengths. Dark horizontal lines that are randomly distributed over the images correspond to stochastic switching of nanorods to the off states because of charge trapping. Whereas this is a good indication that excitation patterns can be attributed to single nanorods, the shape of the patterns corresponds to the case of degeneracy of the excitation dipoles in three dimensions. Excitation isotropy, which indicates the equal probability of exciton generation for the light that is polarized in any of the three dimensions, has been also observed for spherical type-I quantum dots;[13]

DOI: 10.1021/acs.nanolett.8b04695
Nano Lett. XXXX, XXX, XXX–XXX

however, this result is rather unexpected for elongated nanorods with aspect ratios up to 4.

Emission patterns of the same nanorods (Figure 5) have the same shape at all the excitation wavelengths used in this study, do not change with time, and correspond to a fixed linear emission transition dipole. Thus, the emission and excitation transition dipoles have different dimensionalities that remain the same in all the light absorption regimes. The constant shape of both emission and excitation patterns at the time scale of seconds shows that the dimensionality and orientation of both excitation and emission dipoles are not dependent on rapid dynamics processes involving charges. While the excitation isotropy of the excitation transition dipole led to the same pattern of nanorods independent of their orientation, linearity of their emission transition dipole allowed us to measure the three-dimensional orientation of the particles. Figure 5(i) shows histograms of the out-of-plane angles (θ) that were obtained by fitting the emission patterns. The Gaussian fits to the measured data have peaks at 9.7° and 7.0° for 8 × 16 and 8 × 32 nm nanorods, respectively.

Since the roughness of the sample surface did not exceed 1 nm, the nearly horizontal orientation of the emission transition dipole is in agreement with the expectation that it is parallel to the long axis of the elongated particles that lie horizontally on the surface. The deviation from the strictly horizontal orientation is likely related to the partially conical shape of the nanorods that is schematically shown in the inset of Figure 5(i) and that is evident from the transmission electron images of the particles (Figure 1a,b). The difference in the Gaussian peaks maxima position is also in agreement with the assumption that the more elongated 8 × 32 nm nanorods tend to have a slightly lower tilt as compared with 8 × 16 nm ones. A relatively narrow angular distribution of nanorods' out-of-plane orientation (14.8° and 6.3° full width at half maxima for 8 × 16 and 8 × 32 nm nanorods, respectively) indicates monodispersity of the particles.

In summary, we have shown that ZnSe/CdS nanorods have a fixed linear emission and 3D degenerate excitation transition dipole moments. The dimensionality of the transition dipole has neither changed at different aspect ratios of the nanoparticles nor at different excitation wavelengths that correspond to different regimes of light absorption. The excitation isotropy that was also observed in recent studies of spherical CdSe/ZnS quantum dots[13] and CdSe/CdS nanoplatelets,[15] suggesting that it is a common property of semiconductor nanostructures independently on their shape and band gap structure. The linearity of the emission transition dipole moment shows that as for type-I semiconductor nanocrystals,[20] it is determined by the shape of the particles. However, independence of the emission transition dipole dimensionality on the regime of light absorption suggests that fast thermalization of charges after exciton generation leads to their loss of memory of the absorption mode and, as a result, to decoupled absorption and emission polarizations.

■ ASSOCIATED CONTENT

Supporting Information

The Supporting Information is available free of charge on the ACS Publications website at DOI: 10.1021/acs.nanolett.8b04695.

More details regarding the experimental methods and synthesis of ZnSe/CdS nanorods (PDF)

■ AUTHOR INFORMATION

Corresponding Author

*E-mail: alexey.chizhik@phys.uni-goettingen.de.

ORCID

Gaoling Yang: 0000-0003-2218-1781
Narain Karedla: 0000-0002-7891-3825
Ingo Gregor: 0000-0002-1775-2159
Dan Oron: 0000-0003-1582-8532
Jörg Enderlein: 0000-0001-5091-7157
Alexey I. Chizhik: 0000-0003-0454-5924

Notes

The authors declare no competing financial interest.

■ ACKNOWLEDGMENTS

Financial support from the German Science Foundation (DFG, SFB 937, project A14) is gratefully acknowledged. This research was supported by DARPA (fund no. D14PC00141), the European Research Council (ERC) (NVS 669941), and the Human Frontier Science Program (HFSP) (RGP0061/2015). N.K. is grateful for the HFSP postdoctoral fellowship. This work was also supported by STROBE, a National Science Foundation Science & Technology Center (DMR 1548924).

■ REFERENCES

(1) Park, K.; Kuo, Y.; Shvadchak, V.; Ingargiola, A.; Dai, X.; Hsiung, L.; Kim, W.; Zhou, Z. H.; Zou, P.; Levine, A. J.; Li, J.; Weiss, S. *Science Advances* **2018**, *4*, No. e1601453.

(2) Park, K.; Deutsch, Z.; Li, J. J.; Oron, D.; Weiss, S. *ACS Nano* **2012**, *6*, 10013−10023.

(3) Bar-Elli, O.; Steinitz, D.; Yang, G.; Tenne, R.; Ludwig, A.; Kuo, Y.; Triller, A.; Weiss, S.; Oron, D. *ACS Photonics* **2018**, *5*, 2860−2867.

(4) Marshall, J. D.; Schnitzer, M. J. *ACS Nano* **2013**, *7*, 4601−4609.

(5) Kuo, Y.; Li, J.; Michalet, X.; Chizhik, A.; Meir, N.; Bar-Elli, O.; Chan, E.; Oron, D.; Enderlein, J.; Weiss, S. *ACS Photonics* **2018**, *5*, 4788−4800.

(6) Klimov, V. I.; Ivanov, S. A.; Nanda, J.; Achermann, M.; Bezel, I.; McGuire, J. A.; Piryatinski, A. *Nature* **2007**, *447*, 441−446.

(7) Efros, A. L. *Phys. Rev. B: Condens. Matter Mater. Phys.* **1992**, *46*, 7448−7458.

(8) Empedocles, S. A.; Neuhauser, R.; Bawendi, M. G. *Nature* **1999**, *399*, 126−130.

(9) Empedocles, S. A.; Neuhauser, R.; Shimizu, K.; Bawendi, M. G. *Adv. Mater.* **1999**, *11*, 1243−1256.

(10) Patra, D.; Gregor, I.; Enderlein, J. *J. Phys. Chem. A* **2004**, *108*, 6836−6841.

(11) Brokmann, X.; Coolen, L.; Dahan, M.; Hermier, J. P. *Phys. Rev. Lett.* **2004**, *93*, 107403.

(12) Schuster, R.; Barth, M.; Gruber, A.; Cichos, F. *Chem. Phys. Lett.* **2005**, *413*, 280−283.

(13) Chizhik, A. I.; Chizhik, A. M.; Khoptyar, D.; Bär, S.; Meixner, A. J. *Nano Lett.* **2011**, *11*, 1131−1135.

(14) Sitt, A.; Hadar, I.; Banin, U. *Nano Today* **2013**, *8*, 494−513.

(15) Ma, X.; Diroll, B. T.; Cho, W.; Fedin, I.; Schaller, R. D.; Talapin, D. V.; Wiederrecht, G. P. *Nano Lett.* **2018**, *18*, 4647−4652.

(16) Dedecker, P.; Muls, B.; Deres, A.; Uji-i, H.; Hotta, J.-i.; Sliwa, M.; Soumillion, J.-P.; Müllen, K.; Enderlein, J.; Hofkens, J. *Adv. Mater.* **2009**, *21*, 1079−1090.

(17) Ghosh, S.; Chizhik, A. M.; Karedla, N.; Dekaliuk, M. O.; Gregor, I.; Schuhmann, H.; Seibt, M.; Bodensiek, K.; Schaap, I. A. T.; Schulz, O.; Demchenko, A. P.; Enderlein, J.; Chizhik, A. I. *Nano Lett.* **2014**, *14*, 5656−5661.

(18) Dorfs, D.; Salant, A.; Popov, I.; Banin, U. *Small* **2008**, *4*, 1319−1323.

DOI: 10.1021/acs.nanolett.8b04695
Nano Lett. XXXX, XXX, XXX−XXX

(19) Oron, D.; Kazes, M.; Banin, U. *Phys. Rev. B: Condens. Matter Mater. Phys.* **2007**, *75*, 035330.
(20) Hu, J.; Li, L.-s.; Yang, W.; Manna, L.; Wang, L.-w.; Alivisatos, A. P. *Science* **2001**, *292*, 2060−2063.

DOI: 10.1021/acs.nanolett.8b04695
Nano Lett. XXXX, XXX, XXX−XXX